JPPIPA 10(8) (2024)

Jurnal Penelitian Pendidikan IPA

Journal of Research in Science Education

http://jppipa.unram.ac.id/index.php/jppipa/index

Implementation of the Gauss-Kronrod Quadrature Method (G7, K15) on 2D Gravity Anomaly Modeling in Basins with a Polynomial Variation of Density Distribution with Depth

Zulhendra[1*], Wahyu Srigutomo[2], Cahyo Aji Hapsoro[3]

[1] Department of Physics, Faculty of Mathematics and Natural Science, Universitas Negeri Padang, Padang, Indonesia.
[2] Department of Physics, Faculty of Mathematics and Natural Science, Institut Teknologi Bandung, Bandung, Indonesia.
[3] Department of Physics, Faculty of Mathematics and Natural Science, Universitas Negeri Semarang, Malang, Indonesia.

Received: June 17, 2024
Revised: July 12, 2024
Accepted: August 25, 2024
Published: August 31, 2024

Corresponding Author:
Zulhendra
zulhendra@fmipa.unp.ac.id

DOI: 10.29303/jppipa.v10i8.8493

Abstract: Forward modeling of 2D gravity anomalies, considering density contrasts that vary polynomially with depth, was performed to examine basin structures. This process involved two main stages: deriving analytical formulas and executing numerical integration. The Gauss-Kronrod Quadrature Method, utilizing 7 Gauss points and 15 Kronrod points, was employed to precisely compute these integrals. Initial modeling applied to theoretical basement scenarios with fixed density contrasts showed gravity anomalies that accurately reflected the curvature of the basement. To validate the approach, it was then applied to real-world cases including the Sebastian Vizcaino Basin, San Jacinto Graben, and Sayula Basin. By incorporating suitable density contrasts, modeling lengths, and basement curvature shapes, the results revealed that both fixed-density and depth-variable density models produced gravity anomalies with patterns consistent with the actual basement curvature. These findings validate the modeling technique's effectiveness in representing real geological features accurately. The study confirms that the Gauss-Kronrod Quadrature Method (G7, K15) is robust for analyzing 2D gravity anomalies, providing a reliable tool for understanding the influence of varying density contrasts on gravity responses.

Keywords: Basin; Gauss-Kronrod quadrature; Gravity anomaly; Variation of density

Introduction

Gravity anomaly modeling is a crucial geophysical technique used to explore the Earth's subsurface structure. These anomalies, which result from differences between the measured gravitational acceleration at the Earth's surface and the expected values from a homogeneous Earth model, provide vital insights for geological mapping, identifying disaster zones such as liquefaction (Silalahi et al., 2023), exploring natural resources such as geothermal structures (Larasati et al., 2023) and analyzing regional Earth dynamics. and regional Earth dynamics analysis. The variations in the gravitational field that lead to these anomalies are caused by differences in the mass of the Earth's crust.

Sedimentary basins, often characterized by negative gravity anomalies, are of particular economic importance. These basins are essential sources of energy-related products such as oil, gas, coal, uranium, and geothermal fluids, and they also serve as major depositional reservoirs for various minerals (Oksum, 2021). The negative gravity anomalies observed over these basins typically result from the lower density of the sedimentary rocks filling the basin compared to the denser basement rocks beneath them (Chakravarthi et al., 2016). This density generally increases with depth due to processes like mechanical compaction and diagenesis, which raise sediment density and reduce

How to Cite:
Zulhendra, Srigutomo, W., & Hapsoro, C. A. (2024). Implementation of the Gauss-Kronrod Quadrature Method (G7, K15) on 2D Gravity Anomaly Modeling in Basins with a Polynomial Variation of Density Distribution with Depth. *Jurnal Penelitian Pendidikan IPA*, *10*(8), 6252–6259. https://doi.org/10.29303/jppipa.v10i8.8493

porosity (Cai & Zhdanov, 2015; Chappell & Kusznir, 2008; Tenzer & Gladkikh, 2014).

Many existing algorithms use stacked prism models to analyze sedimentary basin gravity anomalies (Abdoh et al., 1990; Bott, 1960; İşseven et al., 2024) and complex contour integrals (Kwok, 1991). The technique developed by Annecchione et al. (2001) is based on the assumption that the sediment load above the bed has a uniform density. Understanding the relationship between rock density and depth is crucial for delineating basin boundaries and assessing the depth distribution of sedimentary basins, which plays a vital role in hydrogeological studies and resource management (Abbott & Louie, 2000; Chakravarthi et al., 2016; Chakravarthi & Sundararajan, 2005, 2007; Himi et al., 2017; Lekula et al., 2018). Various mathematical formulations have been developed to model subsurface mass distribution, including exponential (Chappell & Kusznir, 2008; Cordell, 1973; Cowie & Karner, 1990; Granser, 1987; Rao, 1990), hyperbolic (Litinsky, 1989; Silva et al., 2006), parabolic (Roy & Wu, 2023), and polynomial models (D'Urso, 2015; García-Abdeslem, 1996, García-Abdeslem, 2003; García-Abdeslem et al., 2005; Srigutomo et al., 2018).

In this study, we will apply the Gauss-Kronrod Quadrature G7, K15 method to model 2D gravity anomalies in basins with polynomial density distributions with depth. This approach introduces a more robust numerical framework for handling the complexities of density variations in geophysical contexts. While previous studies have employed various mathematical approaches to describe density-depth relationships, the Gauss-Kronrod Quadrature method stands out for its enhanced accuracy in numerical integration, which is critical for modeling complex subsurface structures. By offering greater precision in gravity anomaly modeling, this method facilitates more accurate interpretations of subsurface structures, which is crucial for effective exploration and management of natural resources, particularly in sedimentary basins. The introduction of this method not only addresses the limitations of previous approaches but also advances the field of geophysical modeling, providing new perspectives on managing complex subsurface density distributions. Ultimately, this research aims to significantly improve the accuracy and reliability of subsurface modeling, thereby deepening our understanding of the Earth's subsurface and its resource potential.

Method

Figure 1 illustrates the cross-section of a sedimentary basin. The source body, situated between x1 and x2, is divided into M segments. These segments are located within the source body Ω, either on the vertical lines of the segments or between them, and are confined by the functions h1(x) and h2(x). The density contrast along the segment body changes vertically with depth according to a polynomial equation (García-Abdeslem, 2003).

$$\rho(z) = p + qz + rz^2 + sz^3 \quad (1)$$

where p, q, r, and s are the coefficients describing the density contrast as a function of depth.

The gravitational anomaly of each segment, $g(x_0, z_0)$, at each observation point, $P(x_0, z_0)$, on the profile between x1 and x1, enclosed within a region Ω, follows the formulation (García-Abdeslem, 2003).

$$g_{seg}(x_0, z_0) = 2\gamma \iint_{\Omega} dxdy \frac{\rho(z)Z}{X^2+Z^2} \quad (2)$$

where γ is Newton's gravitational constant. Here, X = x − x_0, Z = z − z_0, and (x, z) denote the coordinates of a material point within the region.

Equation 2 is solved García-Abdeslem (2003) in two steps: first, by analytically solving the z-dependent integral

$$g_{seg}(x_0, z_0) = \int_{x1}^{x2} dx\, 2\gamma \left\{ \int_{h_1(x)}^{h_2(x)} \frac{\rho(z)Z}{X^2+Z^2} \right\} \quad (3)$$

Performing the integration along the z-direction yields

$$g_{seg}(x_0, z_0) = 2\gamma \int_{x1}^{x2} dx \left\{ \frac{1}{2} [\rho(z_0) - [r + 3sz_0]X^2] \times ln(X^2 + Z^2) + [sX^2 - \rho'(z_0)]Xarctan\left(\frac{Z}{X}\right) + [\rho'(z_0) - sX^2]Z + \frac{(r+3sz_0)Z^2}{2} + \frac{sZ^3}{3} \right\} \Big|_{h_1(x)}^{h_2(x)}, \quad (4)$$

Where $\rho'(z_0) = q + 2rz_0 + 3sz_0^2$ is the depth derivative of the density function evaluated at z = z_0.

In the case of a land survey, h1(x) describes the topographic relief, and the gravity station is positioned above it so that h1(x) → z_0. Consequently, the integral in equation (4) becomes singular. To avoid singularities in such cases, the integration interval is divided around the gravity station location. Furthermore, by substituting the coefficients of the density-depth function in equation (4) with functions of the variable x, the density function can be modified to account for density variations along the x and z directions:

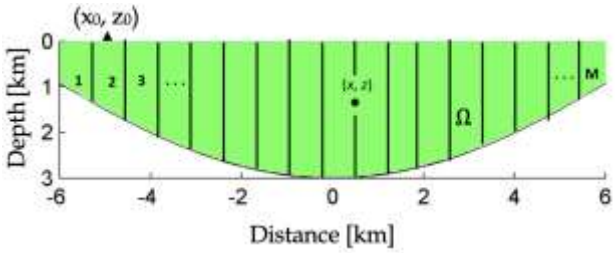

Figure 1. Illustration of the source body partition into M segments (Srigutomo et al., 2018)

$$\rho(x,z) = p(x) + q(x)z + r(x)z^2 + s(x)z^3 \quad (5)$$

These must be continuous functions, such as polynomials or circular functions. This approach allows for the conversion of a velocity field into a density field using empirical velocity–density relationships, which can be useful for geological stripping (García-Abdeslem, 2003).

In this study, equation 4 is solved numerically using the Gauss-Kronrod Quadrature Method (Alqahtani et al., 2024; Kronrod, 1965; Laurie, 1997; Notaris, 2016; Oishi & Sakamoto, 2017). The Gauss-Kronrod quadrature formula is an adaptive technique for numerical integration. It is a variation of Gaussian quadrature where the evaluation points are selected to allow for an accurate approximation by reusing information from a less precise approximation. This method exemplifies a nested quadrature rule: it employs the same set of function evaluation points to create two quadrature rules, one of higher order and one of lower order (known as the embedded rule). The difference between these two approximations helps estimate the computational error of the integration.

The challenge in numerical integration is to approximate definite integrals of the form:

$$\int_{x_1}^{x_2} f(x)dx \quad (6)$$

Such integrals can be approximated using n-point Gaussian quadrature as follows:

$$\int_1^{-1} f(x)dx \approx \sum_{i=1}^{n} w_i f(x_i) \quad (7)$$

where w_i and x_i are the weights and points at which the function f(x).

When the interval [x1, x2] is subdivided, the Gauss evaluation points of the new subintervals do not match the previous evaluation points (except at the midpoint for an odd number of points), requiring the integrand to be evaluated at every point. The Gauss-Kronrod formulas extend the Gauss quadrature formulas by adding n+1 points to an n-point rule, resulting in a rule of order 3n+1 (while the corresponding Gauss rule is of order 2n-1). These additional points are the zeros of Stieltjes polynomials, enabling higher-order estimates while reusing function values from lower-order estimates. The difference between a Gauss quadrature rule and its Kronrod extension is often used to estimate the approximation error.

In this study, the 7-point Gauss rule was combined with the 15-point Kronrod rule which can be seen in Table 1. Since the Gauss points are included in the Kronrod points, only 15 function evaluations are required. The integral is then estimated using the Kronrod rule K15 and the error can be estimated as (G7-K15). For an arbitrary interval [x_1, x_2] the node positions x_i and weights w_i are scaled to the interval as follows:

$$x_i, scale = \frac{x_{i+1}}{2}(x_2 - x_1) + x_1 \quad (8)$$

$$w_i, scale = \frac{w_i}{2}(x_2 - x_1) \quad (9)$$

The total gravity anomaly produced by a basin at any observation point can be obtained as:

$$g_{basin}(x_0, z_0) = \sum_{i=1}^{M} g_{seg}(x_0, z_0) \quad (10)$$

Where M represents the number of segments/ observations on the profile.

Tabel 1. Gauss and Kronrod nodes and weights.

(G7, K15) on [−1,1]		
G7	Gauss nodes	Weights
	±0.949107912342759	0.129484966168870
	±0.741531185599394	0.279705391489277
	±0.405845151377397	0.381830050505119
	0.000000000000000	0.417959183673469
K15	Kronrod nodes	Weights
	±0.991455371120813	0.022935322010529
	±0.949107912342759	0.063092092629979
	±0.864864423359769	0.104790010322250
	±0.741531185599394	0.140653259715525
	±0.586087235467691	0.169004726639267
	±0.405845151377397	0.190350578064785
	±0.207784955007898	0.204432940075298
	0.000000000000000	0.209482141084728

Result and Discussion

The modeling of the source body with a basin-shaped basement was tried for a fixed density contrast to validate the gravity anomaly response using the Gauss-Kronrod Quadrature (G7, K15) calculation method. This aims to see the gravity anomaly response to the source body. Figure 2 shows a simple basin model with basin filling material as the source body that has a

fixed density contrast. The basement topography is made flat, which is expressed by the equation $h_1(x) = 0$, and the Fourier series equation expresses the bedrock geometry in the form of cosine, namely $h_2(x) = 4 + cos2\pi/L$, where L is the modeling length. The density contrast value between the basement and the sediment filling the basin is determined at $-0.7\ Mg/m^3$. Gravity anomalies are calculated on the surface along 80 km with the exact distance between points, as many as 165 points. The resulting gravity anomaly response curves downward with a curve pattern that matches the geometry of the bedrock. The anomaly response generated in this modeling using Gauss-Kronrod Quadrature calculations (G7, K15) has a pattern that matches the calculation using the Gauss Quadrature two-point rule (Srigutomo et al., 2018).

The real problem in the field is the problem of estimating the shape of the bedrock of a basin from gravity anomaly data measured on the surface (Srigutomo et al., 2018). Before the gravity data inversion scheme was developed for this modeling case, a more real density and basement geometry shape was tried, which was taken from several cases of data interpretation from several basins that had been studied.

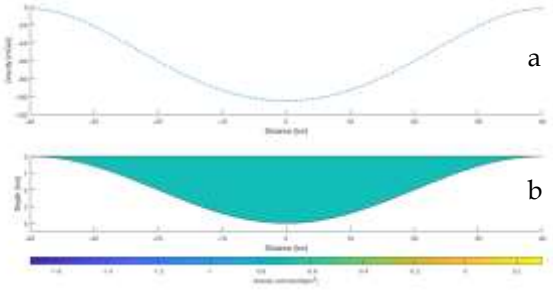

Figure 2. (a) Calculation of gravity anomalies from research results. (b) Basin model with a constant density contrast of $-0.7\ Mg/m^3$.

This is related to thick basins; sedimentary rock density varies with depth, so the assumption of constant density contrast is often unrealistic (Chakravarthi et al., 2016; Florio, 2020; Mallesh et al., 2019). Density contrast with polynomial variation with depth in the Sebastian Vizcaino basin, San Jacinto graben, and Sayula basin is used in modeling to obtain a more realistic real case. The geometric shape of the basement in the modeling follows the geometric shape of the basement of the three basins from previous studies (García-Abdeslem, 2003; García-Abdeslem et al., 2005), which is fitted using a Fourier series following Formula 11.

$$h_2(x) = m_1 + \sum_{i=1}^{14} \mathrm{m_i} \cos\left[\frac{i-1}{Lb}\right] + \sum_{i=1}^{14} \mathrm{m_i} \sin\left[\frac{i-1}{Lb}\right] \qquad (11)$$

The m value used to form the basement geometry for the three basins can be seen in Table 2.

Table 2. Fourier coefficients forming the basement geometry used in the modeling.

Vizcaino (mi)		San Jacinto (mi)		Sayula (mi)	
1.5333	0.8300	0.5857	0.3625	0.2826	0.0612
-1.2484	-0.8405	-0.5401	-0.7074	0.2751	0.1050
0.2631	-0.1194	0.0983	0.2235	0.2138	0.0629
0.1145	-0.1146	-0.0042	0.0429	0.1119	-0.0193
-0.2152	-0.0717	-0.2347	0.0438	0.0596	-0.0368
-0.1465	-0.0253	-0.0145	0.0791	0.0426	-0.0185
-0.0770	0.0554	0.1090	0.0204	0.0094	-0.0172
-0.0204	-0.0025	0.0206	-0.0479	-0.0009	-0.0068
-0.0619	-0.0008	0.0330	-0.0265	0.0126	0.0003
-0.0387	0.0160	0.0011	-0.0121	0.0001	-0.0140
-0.0427	0.0209	-0.0118	-0.0019	-0.0104	-0.0054
-0.0288	0.0268	-0.0133	0.0063	0.0008	0.0104
-0.0228	0.0211	-0.0060	0.0036	-0.0018	-0.0052
-0.0025	0.0108	-0.0009	0.0024	0.0016	0.0010
0.0023		0.0015		-0.0002	

First, the Sebastian Vizcaino basin model, Baja California Sur Mexico. The density contrast of this basin is in the form of $\rho(z) - 0{,}7 + 0{,}2548z - 0{,}0273z^2$ as a result of fitting density data converted from the relationship between density and seismic velocity using a second-order polynomial (García-Abdeslem et al., 2005). The gravity anomaly response shown in Figure 3 is the result of calculations in this study for the shape of the Sebastian Vizcaino basin. The results of this calculation are in accordance with the results of previous research (Cordell, 1973; García-Abdeslem et al., 2005), which used 32-point Gauss Quadrature integrals in calculating gravity anomaly. The modeling in Figure 3 uses the basement curvature from previous research (García-Abdeslem et al., 2005) following the Fourier series in equation (9) and using the coefficient m in Table 2, X1 = 1 km and X2 = 83 km, b = 5, and L = X2 – X1. The calculation results show that the gravity anomaly curvature pattern curves downward and has a negative value in accordance with the geometry of the basement, in accordance with previous research (Srigutomo et al., 2018), which uses a 2-point Gauss Quadrature integral.

Second, the San Jacinto graben with this basin density contrast is in the form of $(z) - 0.5491 + 0.2682z - 0.0581z^2 + 0.0053z^3$. This graben is a transtensional basin formed due to right-side dilational movement that occurred in the San Jacinto fault zone (Matti & Morton, 1993). The gravity anomaly response shown in Figure 4 is the result of calculations in this study for the shape of the San Jacinto graben. The results of this calculation are also in accordance with the results of previous research (García-Abdeslem, 2003), which

uses a 32-point Gauss Quadrature integral in calculating gravity anomalies. The modeling in Figure 4 uses the basement curvature from previous research (García-Abdeslem, 2003) following the Fourier series in equation (9) and using the coefficient m in Table 2, X1 = -0.645 km and X2 = 10.948 km, b = 5, and L = X2 – X1. The curvature of the gravity anomaly response also shows a curvature pattern following the shape of the basement curvature.

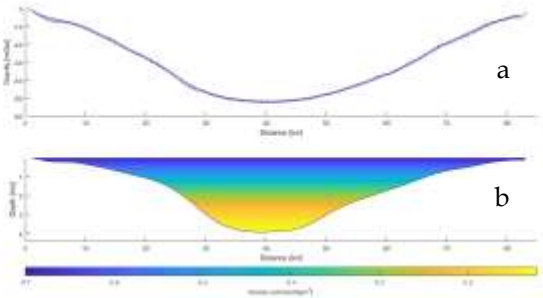

Figure 3. (a) Calculation of gravity anomaly (black circle) from research results and gravity anomaly (blue line) of Sebastian Vizcaino Basin (Garcia et al., 2005). (b) Basement curvature shape of Sebastian Vizcaino Basin (Garcia et al., 2005).

Third, the Sayula Basin with this basin density contrast is in the form of $(z) - 0{,}8 + 0{,}7147z - 0{,}229z^2$. The Sayula area is part of a larger geomorphological unit known as the Tepic-Chapala Graben that contains several tectonic depressions. Over the course of several glacial episodes, heavy rainfall submerged the land and left traces of large lakes (Valdez et al., 2006). The gravity anomaly response shown in Figure 5 is the result of calculations in this study for the shape of the Sayula Basin.

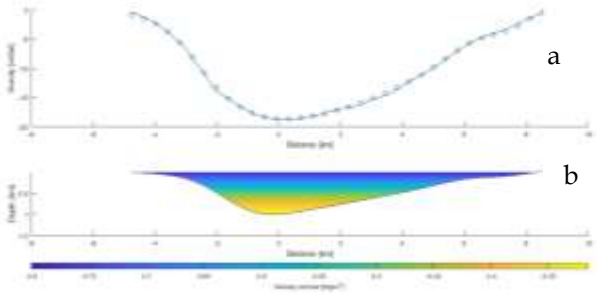

Figure 4. (a) Calculation of gravity anomaly (black circle) from research results and gravity anomaly (blue line) of San Jacinto Graben (García-Abdeslem, 2003). (b) The shape of the curvature of the basement of San Jacinto Graben (García-Abdeslem, 2003).

The results of this calculation are slightly different by two meals at its minimum value from the results of previous research (Chakravarthi & Ramamma, 2015), which used a 32-point Gauss Quadrature integral in calculating gravity anomalies. This was identified as a result of the model lacking in the results of the slightly random gravity data inversion from previous studies, so there was a difference in the calculation of the 32-point Gauss Quadrature integral and Gauss-Cronrod Quadrature (G7, K15). The Gauss-Cronrod Quadrature (G7, K15) integral was able to calculate the gravity anomaly response in the two previous basins, namely the Sebastian Vizcaino Basin and the San Jacinto Graben, which identified the correctness of the calculation. The modeling in Figure 5 uses the basement curvature from previous studies (Chakravarthi & Ramamma, 2015) following the Fourier series in equation (11) and using the coefficient m in table 2, X1 = -0.475 km and X2 = 8.5 km, b = 3, and L = X2 - X1. The curvature of the gravity anomaly response shows a curvature pattern following the shape of the basement curvature.

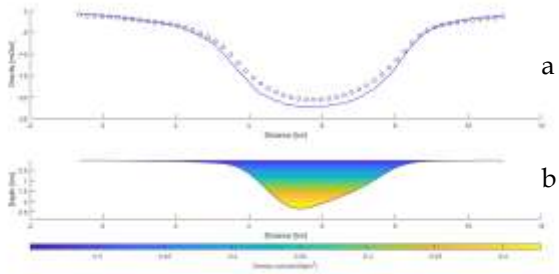

Figure 5. (a) Calculation of gravity anomaly (black circle) from research results and gravity anomaly (blue line) of Sayula Basin (García-Abdeslem, 2003). (b) Curvature shape of Sayula Basin basement (García-Abdeslem, 2003).

Conclusion

Forward modeling of 2D gravity anomalies with density contrasts that vary polynomially with depth was conducted to analyze basin structures. The process involved two key stages: deriving analytical formulas and performing numerical integration. The Gauss-Kronrod Quadrature Method, featuring 7 Gauss points and 15 Kronrod points, was used to accurately compute these integrals. The modeling was first applied to theoretical basement cases with fixed density contrasts, revealing gravity anomalies that corresponded well with the basement's curvature. Subsequently, the approach was validated against real-world cases from the Sebastian Vizcaino Basin, San Jacinto Graben, and Sayula Basin. By using appropriate density contrasts, modeling lengths, and basement curvature shapes, the results demonstrated that both fixed-density and depth-variable density models produce gravity anomalies with curvature patterns consistent with the basement's structure. This confirms the effectiveness of the modeling technique in reflecting real geological features.

Acknowledgments
Thank you to everyone who assisted in this research, enabling the publication of this article.

Author Contributions
Conceptualization, Z., W. S., and C. A. H.; methodology, Z. and W. S.; software, Z. and W. S.; validation, Z., W. S., and C. A. H.; resources, Z. and W. S.; data curation, Z., W. S., and C. A. H.; writing—original draft preparation, Z.; writing—review and editing, Z., W. S. and C. A. H.; visualization, Z. and W. S. All authors have read and agreed to the published version of the manuscript.

Funding
No external funding was received.

Conflicts of Interest
No conflicts of interest.

References

Abbott, R. E., & Louie, J. N. (2000). Depth to bedrock using gravimetry in the Reno and Carson City, Nevada, area basins. *Geophysics*, *65*(2), 340–350. https://doi.org/10.1190/1.1444730

Abdoh, A., Cowan, D., & Pilkington, M. (1990). 3D Gravity Inversion of The Cheshire Basin. *Geophysical Prospecting*, *38*(8), 999–1011. https://doi.org/10.1111/j.1365-2478.1990.tb01887.x

Alqahtani, H., Borges, C. F., Djukić, D. L., Djukić, R. M., Reichel, L., & Spalević, M. M. (2024). Computation of pairs of related Gauss-type quadrature rules. *Applied Numerical Mathematics*. https://doi.org/10.1016/j.apnum.2024.03.003

Annecchione, M. A., Chouteau, M., & Keating, P. (2001). Gravity interpretation of bedrock topography: the case of the Oak Ridges Moraine, southern Ontario, Canada. *Journal of Applied Geophysics*, *47*(1), 63–81. https://doi.org/10.1016/S0926-9851(01)00047-7

Bott, M. H. P. (1960). The use of rapid digital computing methods for direct gravity interpretation of sedimentary basins. *Geophysical Journal International*, *3*(1), 63–67. https://doi.org/10.1111/j.1365-246X.1960.tb00065.x

Cai, H., & Zhdanov, M. (2015). Application of Cauchy-type integrals in developing effective methods for depth-to-basement inversion of gravity and gravity gradiometry data. *Geophysics*, *80*(2), 81– 94. https://doi.org/10.1190/geo2014-0332.1

Chakravarthi, V., Kumar, M. P., Ramamma, B., & Sastry, S. R. (2016). Automatic gravity modeling of sedimentary basins by means of polygonal source geometry and exponential density contrast variation: Two space domain based algorithms. *Journal of Applied Geophysics*, *124*, 54–61. https://doi.org/10.1016/j.jappgeo.2015.11.007

Chakravarthi, V., & Ramamma, B. (2015). Determination of sedimentary basin basement depth: a space domain based gravity inversion using exponential density function. *Acta Geophysica*, *63*, 1066–1079. https://doi.org/10.1515/acgeo-2015-0027

Chakravarthi, V., & Sundararajan, N. (2005). Gravity modeling of 21/2-D sedimentary basins—a case of variable density contrast. *Computers & Geosciences*, *31*(7), 820–827. https://doi.org/10.1016/j.cageo.2005.01.018

Chakravarthi, V., & Sundararajan, N. (2007). INV2P5DSB—A code for gravity inversion of 2.5-D sedimentary basins using depth dependent density. *Computers & Geosciences*, *33*(4), 449–456. https://doi.org/10.1016/j.cageo.2006.06.010

Chappell, A., & Kusznir, N. (2008). An algorithm to calculate the gravity anomaly of sedimentary basins with exponential density-depth relationships. *Geophysical Prospecting*, *56*(2), 249–258. https://doi.org/10.1111/j.1365-2478.2007.00674.x

Cordell, L. (1973). Gravity analysis using an exponential density-depth function—San Jacinto Graben, California. *Geophysics*, *38*(4), 684–690. https://doi.org/10.1190/1.1440367

Cowie, P. A., & Karner, G. D. (1990). Gravity effect of sediment compaction: examples from the North Sea and the Rhine Graben. *Earth and Planetary Science Letters*, *99*(1–2), 141–153. https://doi.org/10.1016/0012-821X(90)90078-C

D'Urso, M. G. (2015). The gravity anomaly of a 2D polygonal body having density contrast given by polynomial functions. *Surveys in Geophysics*, *36*(3), 391–425. https://doi.org/10.1007/s10712-017-9411-9

Florio, G. (2020). The estimation of depth to basement under sedimentary basins from gravity data: Review of approaches and the ITRESC method, with an application to the Yucca Flat Basin (Nevada. *Surveys in Geophysics*, *41*(5), 935–961. https://doi.org/10.1007/s10712-020-09601-9

García-Abdeslem, J. (1996). GL2D: A Fortran program to compute the gravity anomaly of a 2-d prism where density varies as a function of depth. *Computers & Geosciences*, *22*(7), 823–826. https://doi.org/10.1016/0098-3004(96)00020-9

García-Abdeslem, J. (2003). 2D modeling and inversion of gravity data using density contrast varying with depth and source–basement geometry described by the Fourier series. *Geophysics*, *68*(6), 1909–1916. https://doi.org/10.1190/1.1635044

García-Abdeslem, J., Romo, J. M., Gómez-Treviño, E., Ramírez-Hernández, J., Esparza-Hernández, F. J., & Flores-Luna, C. F. (2005). A constrained 2D

gravity model of the sebastián vizcaíno basin. *Geophysical Prospecting*, *53*(6), 755–765. https://doi.org/10.1111/j.1365-2478.2005.00510.x

Granser, H. (1987). Three-dimensional interpretation of gravity data from sedimentary basins using an exponential density-depth function. *Geophysical Prospecting*, *35*(9), 1030–1041. https://doi.org/10.1111/j.1365-2478.1987.tb00858.x

Himi, M., Tapias, J., Benabdelouahab, S., Salhi, A., Rivero, L., Elgettafi, M., & Casas, A. (2017). Geophysical characterization of saltwater intrusion in a coastal aquifer: the case of Martil-Alila plain (North Morocco. *Journal of African Earth Sciences*, *126*, 136–147. https://doi.org/10.1016/j.jafrearsci.2016.11.011

İşseven, T., Aydın, N. G., & Arslan, M. S. (2024). 2D modelling the depth of the southeastern Thrace Basin by using Bouguer gravity anomalies. *Acta Geophysica*, *72*(2), 849–860. https://doi.org/10.1007/s11600-023-01140-2

Kronrod, A. S. (1965). *Nodes and weights of quadrature formulas*. New York: Sixteen-place tables Consultants Bureau.

Kwok, Y. K. (1991). Contour integrals for gravity computation of horizontal 212-D bodies with variable density. *Applied Mathematical Modelling*, *15*(2), 98–103. https://doi.org/10.1016/0307-904X(91)90017-J

Larasati, N. E., Laesanpura, A., & Sugianto, A. (2023). Integrative Analysis of the Geothermal Structure in Kepahiang: Insights from Magnetotelluric, Gravity, and Remote Sensing Techniques. *Jurnal Penelitian Pendidikan*, *9*(8), 5971–5978. https://doi.org/10.29303/jppipa.v9i8.4576

Laurie, D. (1997). Calculation of Gauss-Kronrod quadrature rules. *Mathematics of Computation*, *66*(219), 1133–1145. Retrieved from https://www.ams.org/journals/mcom/1997-66-219/S0025-5718-97-00861-2/

Lekula, M., Lubczynski, M. W., & Shemang, E. M. (2018). Hydrogeological conceptual model of large and complex sedimentary aquifer systems–Central Kalahari Basin. In *Physics and Chemistry of the Earth, Parts A/B/C* (Vol. 106, pp. 47–62). https://doi.org/10.1016/j.pce.2018.05.006

Litinsky, V. A. (1989). Concept of effective density: Key to gravity depth determinations for sedimentary basins. *Geophysics*, *54*(11), 1474–1482. https://doi.org/10.1190/1.1442611

Mallesh, K., Chakravarthi, V., & Ramamma, B. (2019). 3D gravity analysis in the spatial domain: Model simulation by multiple polygonal cross-sections coupled with exponential density contrast. *Pure and Applied Geophysics*, *176*, 2497–2511. https://doi.org/10.1007/s00024-019-02103-9

Matti, J. C., & Morton, D. M. (1993). *Paleogeographic evolution of the San Andreas fault in southern California: A reconstruction based on a new cross-fault correlation*. https://doi.org/10.1130/MEM178-p107

Notaris, S. E. (2016). Gauss-Kronrod quadrature formulae-a survey of fifty years of research. *Electronic Transactions on Numerical Analysis*, *45*, 371–404. Retrieved from https://etna.math.kent.edu/vol.45.2016/pp371-404.dir/pp371-404.pdf

Oishi, Y., & Sakamoto, N. (2017). Numerical computational improvement of the stable-manifold method for nonlinear optimal control. *IFAC-PapersOnLine*, *50*(1), 5103–5108. https://doi.org/10.1016/j.ifacol.2017.08.777

Oksum, E. (2021). Grav3CH_inv: A GUI-based MATLAB code for estimating the 3-D basement depth structure of sedimentary basins with vertical and horizontal density variation. *Computers & Geosciences*, *155*, 104856. https://doi.org/10.1016/j.cageo.2021.104856

Rao, D. B. (1990). Analysis of gravity anomalies of sedimentary basins by an asymmetrical trapezoidal model with quadratic density function. *Geophysics*, *55*(2), 226–231. https://doi.org/10.1190/1.1442830

Roy, A., & Wu, L. (2023). Generalized Gauss-FFT 3D forward gravity modeling for irregular topographic mass having any 3D variable density contrast. *Computers & Geosciences*, *172*, 105297. https://doi.org/10.1016/j.cageo.2023.105297

Silalahi, M. T., Dahrin, D., Abdurrahman, D., & Tohari, A. (2023). Identification of Liquefaction-Potential Zones Using the Gravity Method in Lolu Village Central Sulawesi. *Jurnal Penelitian Pendidikan IPA*, *9*(8), 6206–6212. https://doi.org/10.29303/jppipa.v9i8.4830

Silva, J. B., Costa, D. C., & Barbosa, V. C. (2006). Gravity inversion of basement relief and estimation of density contrast variation with depth. *Geophysics*, *71*(5), 51– 58. https://doi.org/10.1190/1.2236383

Srigutomo, W., Santurima, S., Hapsoro, C. A., Anwar, H., & Djaja, I. G. P. F. S. (2018). Implementation of Two-point Quadrature Gauss-Legendre Method on 2D Gravity Anomaly Modeling in Basins with Density Distribution varied Polynomially as a function of Depth. *Jurnal Geofisika*, *16*(2), 11–18. https://doi.org/10.36435/jgf.v16i2.51

Tenzer, R., & Gladkikh, V. (2014). Assessment of density variations of marine sediments with ocean and sediment depths. *The Scientific World Journal*, *2*(1), 823296. https://doi.org/10.1155/2014/823296

Valdez, F., Emphoux, J. P., Acosta, R., Ramírez, S.,

Reveles, J., & Schöndube, O. (2006). Late Formative archaeology in the Sayula Basin of southern Jalisco. *Ancient Mesoamerica*, *17*(2), 297–311. https://doi.org/10.1017/S0956536106060147